Available online at www.sciencedirect.com
ScienceDirect
Current Applied Physics 8 (2008) 467–470
Current Applied Physics
An official journal of the KPS
www.elsevier.com/locate/cap
www.kps.or.kr

Surface enhanced Raman spectroscopy on nanolithography-prepared substrates

E.C. Le Ru [a,*], P.G. Etchegoin [a], J. Grand [b], N. Félidj [b], J. Aubard [b], G. Lévi [b], A. Hohenau [c], J.R. Krenn [c]

[a] The MacDiarmid Institute for Advanced Materials and Nanotechnology, School of Chemical and Physical Sciences, Victoria University of Wellington, P.O. Box 600, Wellington, New Zealand
[b] Laboratoire ITODYS, Université Paris 7 – Denis Diderot, CNRS UMR 7086, 1 rue Guy de la Brosse, F-75005 Paris, France
[c] Institute of Physics, Karl Franzens University, Universitätsplatz 5, A-8010 Graz, Austria

Available online 1 November 2007

Abstract

In this work, we demonstrate that surface enhanced Raman scattering (SERS) signals allow to track down the localized surface plasmon local field spectral profile of lithographically-designed gold nano-structures. To this purpose, we used rhodamine 6G deposited on various gold nano-particle arrays. The local field spectral profiles obtained are discussed and compared to the far field extinction spectra of the particle arrays. Thus, we show that the normalized relative SERS intensities follow remarkably well the surface plasmon resonances for all the arrays we investigated.

PACS: 78.67.Bf; 33.50.−j; 73.20.Mf; 78.20.Bh

Keywords: Plasmon; Plasmonics; SERS; Metallic surfaces; Local field; Nanolithography

1. Introduction

Surface enhanced Raman scattering (SERS) allows the detection of molecules adsorbed on noble metal substrates (Ag, Au, Cu, etc.) at sub-micro molar concentrations [1,2]. A wide variety of substrates exhibit SERS; among them: electrochemically modified electrodes [3], colloids [4], island films [5–7], particles grafted on silanized glasses [8], and (more recently) regular particle arrays [9,10]. SERS arises from a huge enhancement of the local electromagnetic field close to metallic surfaces, due to the excitation of localized surface plasmons (LSP) [1,2]. LSP manifest themselves in optical resonances (LSPR hereafter), whose frequency is highly dependent on the size/shape of the particles, the inter-particle distance, and the surrounding medium [11]. LSP excitations lead to resonances in the visible and near infra-red (NIR) regions for both far-field (e.g. light absorption), and local field effects (e.g. SERS enhancements). The most common characterization of LSP-supporting structures is optical extinction; a *far-field* property. But it is also desirable to characterize their *local field* properties, and the enhancement in particular. To this end, it is possible to use near-field optics techniques, but these are not as straightforward as extinction measurements. We propose and demonstrate here that the (far-field) measurement of SERS signals can be used to probe the local field properties of LSP-supporting structures. The use of well-defined nanolithographic structures enables also a better understanding of SERS itself. Hence, we highlight the symbiotic relationship

* Corresponding author.
E-mail addresses: Eric.LeRu@vuw.ac.nz (E.C. Le Ru), Pablo.Etchegoin@vuw.ac.nz (P.G. Etchegoin).

1567-1739/$ - see front matter © 2007 Elsevier B.V. All rights reserved.
doi:10.1016/j.cap.2007.10.073

between two distinct and active research areas: SERS and nano-plasmonics.

More precisely, we show experimentally that SERS measurements of a molecular probe (Rhodamine 6G (RH6G)) in these substrates allow us to characterize the surface plasmon resonances and their local field properties. The variations in SERS signals among samples show evidence of an underlying surface plasmon resonance which we change by using regular particle arrays designed by electron beam lithography. These substrates are well-defined samples to study the electromagnetic enhancement mechanism in SERS. Indeed, the localized plasmon resonances, which are at the origin of visible-NIR extinction spectra and the SERS effect, can be tuned to any desired wavelength by varying the particle shape/size and spacing, thus tunning the Raman amplification.

2. Experimental details

Samples were prepared by electron beam lithography (EBL) [12]. After production, SEM and atomic force microscopy (AFM) were used to check the shape, lateral size and height of the particles. Far field properties were characterized from extinction spectra using a micro photospectrometer consisting of a spectrometer (Lot Oriel 260*i*), coupled to an optical microscope (Olympus BX51) equipped with a 50× objective of 0.55 numerical aperture. Arrays with various shapes and dimensions were fabricated, thus resulting in a range of various LSP resonances across the visible. Five arrays with different LSP's were selected for this study, with resonances spanning the region of interest for Raman and SERS at 633 nm excitation: gold nano-triangles with a side length of $a = 100$ nm, a grating constant of $\Lambda = 350$ nm, and a height of $h = 40$ nm (array A); gold nano-triangles with a side length of $a = 150$ nm, a grating constant of $\Lambda = 350$ nm and a height of $h = 40$ nm (array B); gold nano-dots with a diameter of $a = 100$ nm, a grating constant of $\Lambda = 350$ nm, and a height of $h = 40$ nm (array C); gold nano-squares with a side length of $a = 120$ nm, a grating constant of $\Lambda = 350$ nm, and a height of $h = 40$ nm (array D); gold nano-triangles with a side length of $a = 200$ nm, a grating constant of $\Lambda = 350$ nm, and a height of $h = 40$ nm (array E). Fig. 1a–c shows the SEM images of arrays C (dots) and D (squares) and E (triangles), while Fig. 1d shows the extinction spectra of all arrays (A–E) yielding different LSP characteristics. Arrays C and D, for instance, display a single LSP band attributed to the dipolar mode, well described in the literature. Array E clearly reveals two well separated extinction bands at 796 nm and 596 nm.

The high uniformity of these EBL substrates is a major asset for systematic SERS studies. It enables us to probe larger areas with smaller power densities and obtain spectra that are highly reproducible, with no spectral or intensity fluctuations. SERS experiments were performed on a Raman microscope (Jobin Yvon) with a 50× objective using a HeNe laser (633 nm). RH6G was deposited by dipping the substrate in a dye solution (1 μM), and then dried with N_2.

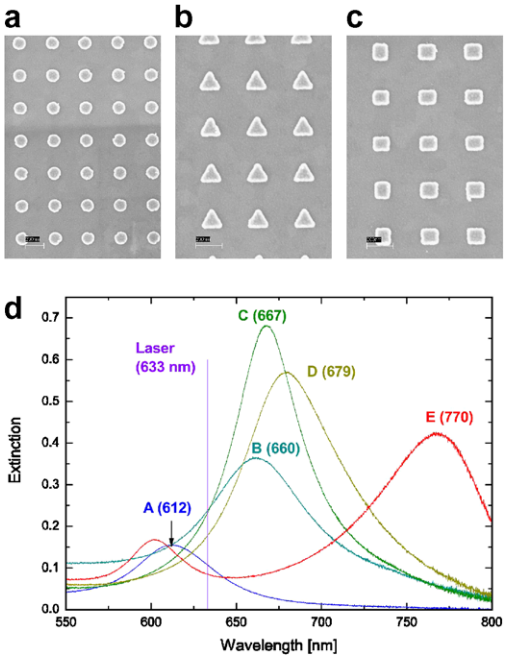

Fig. 1. SEM images of the gold particle arrays: (a) C (dots), (b) E (triangles) and (c) D (squares). (d) Extinction spectra (recorded in air) of the arrays investigated here. The wavelength at the relevant resonance (in nm) is indicated in brackets.

3. Results, discussion, and conclusions

We suggested recently that SERS spectral fluctuations in Ag colloidal aggregates were the result of the underlying spectral dependence of LSP resonances of the aggregates, constantly moving through the scattering volume [13]. Comparing an individual event to the average SERS signals enabled us to track down the LSPR profile corresponding to particular events. Unfortunately, due to the intrinsic non-uniformity of colloidal solutions, it is not possible to correlate an individual LSPR spectral profile with its far-field properties. In this work, the use of well-defined lithographic nano-structures allows us to make this connection, further supporting the interpretations in Ref. [13]. We focus here on arrays of single (non-interacting) nano-particles. We expect in this case that the local field spectral dependence will follow, at least qualitatively, the extinction spectrum, thus enabling us to validate the method. This is not the case in coupled or interacting particles, where the correlation between extinction and local field enhancements is less obvious [16].

To extract information on the local field enhancement, it is useful to write the SERS intensity as:

$$I_{\mathrm{SERS}} \approx M_{\mathrm{Loc}}(\omega_{\mathrm{L}}) M_{\mathrm{Loc}}(\omega_{\mathrm{R}}) I_{\mathrm{RS}}(\omega_{\mathrm{L}}, \omega_{\mathrm{R}}), \quad (1)$$

where $M_{\mathrm{Loc}}(\omega)$ is the local field intensity enhancement factor at frequency ω, ω_{L} (ω_{R}) is the laser (Raman) frequency, and $I_{\mathrm{RS}}(\omega_{\mathrm{R}})$ is the non-enhanced intensity of the Raman

mode. Note that (1) is an approximation, whose conditions of validity are discussed in Ref. [14]. $M_{\mathrm{Loc}}(\omega)$ can then be deduced from I_{SERS}, either by varying ω_{L} for a fixed ω_{R} (a difficult experiment requiring a tunable laser [15]), or by fixing ω_{L} and varying ω_{R}. The latter approach is used here; ω_{R} is "varied" by studying the different Raman modes of the probe. For RH6G at 633 nm excitation, we consider Raman peaks ranging from 612 to 1650 cm^{-1}, resulting in a wavelength range from 658 to 707 nm (this could be extended by using other combinations of laser lines and probes).

SERS spectra were recorded in the arrays and examples are presented in Fig. 2a. The total SERS signal varies among samples due to the different coupling of the laser to the LSP, i.e. to $M_{\mathrm{Loc}}(\omega_{\mathrm{L}})$. The SERS spectra contain two distinct features: a broad background, with a spectral shape which depends on the array and the probe molecule, and Raman peaks. The interpretation of this so-called SERS continuum is still a subject of controversy, and will be discussed elsewhere. In addition, the SERS peaks that "stand out" from the background can be accurately quantified by fitting; their intensities are denoted $I^J(\omega_{\mathrm{R}})$ where $J = \mathrm{A},\ldots,\mathrm{E}$ represents the array, and ω_R the energy of the Raman peak (seven peaks here). It is clear from Eq. (1) that these intensities must contain information about $M_{\mathrm{Loc}}(\omega_{\mathrm{R}})$, which we will now demonstrate. Already in Fig. 2a, we note qualitatively that the ratio between two Raman peaks, like the 612 and 1511 cm^{-1}, varies significantly from one array (A) to the other (E). In fact, the low energy modes are strongly favored over the high energy modes for array A, while the opposite occurs for array E. This is exactly what is expected if the local field spectral dependence follows qualitatively the extinction profile (LSPR for A is at -530 cm^{-1}, while it is at 2810 cm^{-1} for E).

More specifically, we would like ideally to extract $M^J_{\mathrm{Loc}}(\omega_{\mathrm{R}})$ for each array from $I^J(\omega_{\mathrm{R}})$ using Eq. (1). We focus here on the spectral profile of $M^J_{\mathrm{Loc}}(\omega_{\mathrm{R}})$, not its magnitude, so we can ignore the terms that do not depend on ω_{R}, such as $M^J_{\mathrm{Loc}}(\omega_{\mathrm{L}})$. To this end, instead of considering the SERS intensities, we focus on the relative SERS intensities for each array, defined as $R^J(\omega_{\mathrm{R}}) = I^J(\omega_{\mathrm{R}})/\sum_{\omega'_{\mathrm{R}}} I^J(\omega'_{\mathrm{R}})$, where the denominator is the sum of the integrated SERS intensities over all the Raman peaks; this is plotted in Fig. 2b for the seven Raman peaks. Arrays A to E (in increasing order of resonance wavelength) are represented on the x-axis. This figure confirms, on more quantitative grounds, the previous conclusion: the relative contribution of the low energy Raman peaks to the total SERS intensity decreases continuously when the LSPR resonance of the array red-shifts from -530 cm^{-1} (array A) to 2810 cm^{-1} (array E). The opposite happens for high energy peaks, while other peaks show an intermediate behavior. This is a strong indication that the variation of $R^J(\omega_{\mathrm{R}})$ for a given array directly reflects its local field profile. The final step to actually deduce $M^J_{\mathrm{Loc}}(\omega_{\mathrm{R}})$ is to compare the measured $R^J(\omega_{\mathrm{R}})$ to its normal value, $R^0(\omega_{\mathrm{R}})$, i.e. the relative SERS intensities in the absence of local field enhancement. We recall that $\sum_{\omega_{\mathrm{R}}} R^J(\omega_{\mathrm{R}}) = 1$, and as shown in Fig. 2b, that the $R^J(\omega_{\mathrm{R}})$ can be larger or smaller than $R^0(\omega_{\mathrm{R}})$ depending on where the LSP resonance peaks). Since the resonances of our five arrays span a large wavelength range (on both sides of the ω_{R}'s of the Raman peaks, we assume that $R^0(\omega_{\mathrm{R}})$ is simply the average of the $R^J(\omega_{\mathrm{R}})$'s for $J = \mathrm{A},\ldots,\mathrm{E}$. Because the five arrays have very different resonances, we here implicitly assume that the average as defined above "washes out" the spectral dependence and is effectively equivalent to a flat resonance profile. From there, we define the normalized relative SERS intensities $N^J(\omega_{\mathrm{R}}) = R^J(\omega_{\mathrm{R}})/R_0(\omega_{\mathrm{R}})$. This quantity should then be directly proportional to $M_{\mathrm{Loc}}(\omega_{\mathrm{R}})$ and although it does not render any information on its magnitude, it is a direct representation of its spectral profile.

The $N^J(\omega_{\mathrm{R}})$ for each array are plotted vs. the Raman shift in Fig. 3a and can be compared to the corresponding extinction profiles in Fig. 3b. The comparison between the two plots clearly reveals that $N^J(\omega_R)$ follow the LSP resonance profile. This supports our argument that the local field properties can be extracted from the SERS spectra, and also confirms *a posteriori* that the local field profile follows the same qualitative wavelength dependence as the extinction for these single-particle arrays.

Finally, another approach to determine $R^0(\omega_{\mathrm{R}})$ is to directly measure it, which we attempted by recording a

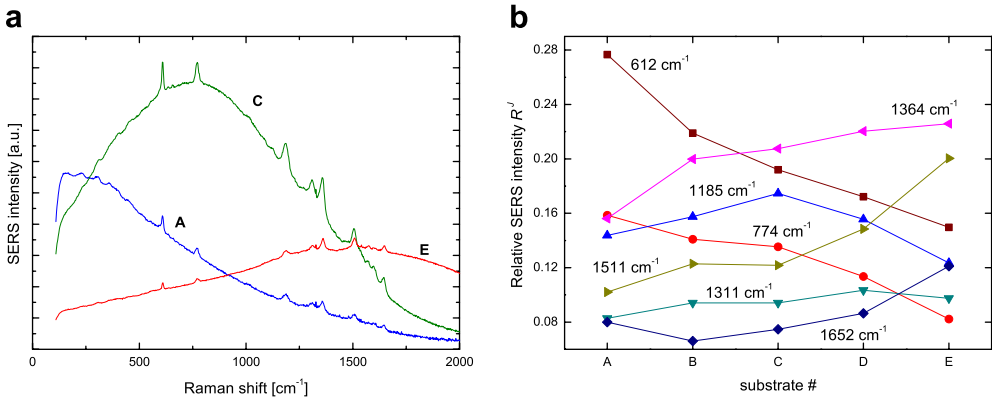

Fig. 2. (a) SERS spectra of RH6G on arrays A, C, and E. (b) Variation of the relative SERS intensities of the main SERS peaks of RH6G for our five arrays whose LSPR wavelengths redshift when moving from A to E.

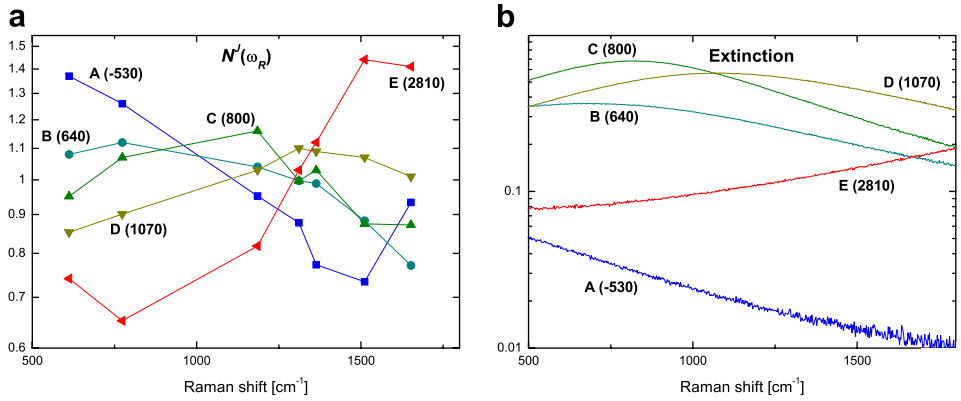

Fig. 3. (a) Normalized relative SERS intensities $N^J(\omega_R)$ (see text), for each array, and (b) extinction spectra of arrays A to E, plotted here versus the Raman shift for direct comparison (LSPR wavenumber in brackets in cm^{-1}).

Raman (non-SERS) spectrum of a pure solution of RH6G (not shown). The measured $R^0(\omega_R)$ (in solution) may however be different to that of RH6G in air, and more importantly to that of RH6G adsorbed on Au (because of metal/molecule interactions and/or of surface selection rules [1]). The approach here gives results similar to that presented above (not shown), except for the 1185 cm^{-1} which appears to be more intense than predicted in all arrays by a factor of ~2. This is a strong indication that the Raman intensity of this particular mode is strongly (enhanced) upon adsorption on gold surfaces, by a mechanism acting in addition to the local field enhancement. Such an observation is the first step towards gaining a better understanding of the adsorption geometry or chemical interaction of the molecule with the metal surface.

This final remark perfectly epitomizes the message we are trying to convey in this work: SERS is a great tool to probe the local field properties of well-defined nano-structures, and this was illustrated here using a particular combination of EBL samples and a SERS probe. This careful characterization, in return, provides additional opportunities to deepen our understanding of the fundamentals of the SERS effect itself, the SERS probe, and the plasmonic properties of metallic substrates, thus paving the way ultimately for the engineering of better SERS substrates for applications.

Acknowledgement

This work was supported by the Dumont d'Urville France/New Zealand exchange programme.

References

[1] R.K. Chang, T.E. Furtak (Eds.), Surface-enhanced Raman-Scattering, Plenum Press, New York, 1982;
M. Moskovits, Rev. Mod. Phys. 57 (1985) 783;
R. Aroca, Surface Enhanced Vibrational Spectroscopy, Wiley, Chichester, 2006.
[2] M. Kerker, D.-S. Wang, H. Chew, Appl. Opt. 19 (1980) 3373;
P.K. Aravind, A. Nitzan, H. Metiu, Surf. Sci. 110 (1981) 189;
S.L. McCall, P.M. Platzman, P.A. Wolf, Phys. Lett. 77A (1980) 381;
J. Gersten, A. Nitzan, J. Chem. Phys. 73 (1980) 3023;
R. Ruppin, Solid State Commun. 39 (1981) 903.
[3] D.L. Jeanmaire, R.P. van Duyne, J. Electroanal. Chem. 84 (1977) 1.
[4] J.A. Creighton, C.G. Blatchford, M.G. Albrecht, J. Chem. Soc. Faraday Trans. 75 (1980) 790.
[5] P.F. Liao et al., Chem. Phys. Lett. 82 (1981) 355.
[6] D.A. Weitz, S. Garoff, T.J. Gramila, Opt. Lett. 7 (1982) 168.
[7] D.A. Weitz, S. Garoff, J.I. Gersten, A. Nitzan, J. Chem. Phys. 79 (1983) 5324.
[8] R.G. Freeman et al., Science 267 (1995) 1629.
[9] N. Félidj et al., Phys. Rev. B 66 (2002) 245407;
L. Gunnarsson et. al, Appl. Phys. Lett. 78 (2001) 802;
M. Kahl, E. Voges, Phys. Rev. B 61 (2000) 14078.
[10] N. Félidj et al., Phys. Rev. B 65 (2002) 75419.
[11] A. Otto, J. Raman Spectrosc. 22 (1991) 743;
F.R. Aussenegg, M.E. Lippitsch, Chem. Phys. Lett. 59 (1978) 214.
[12] M.A. McCord, M.J. Rooks, P. Rai-Choudhury (Eds.), Handbook of Microlithography, Micromachining and Microfabrication, vol. 2, SPIE and The Institution of Electrical Engineers, 1997, pp. 139–249.
[13] E.C. Le Ru, M. Dalley, P.G. Etchegoin, Curr. Appl. Phys. 6 (2006) 411.
[14] E.C. Le Ru, P.G. Etchegoin, Chem. Phys. Lett. 423 (2006) 63.
[15] A.D. McFarland, M.A. Young, J.A. Dieringer, R.P. Van Duyne, J. Phys. Chem. B 109 (2005) 11279.
[16] E.C. Le Ru, C. Galloway, P.G. Etchegoin, Phys. Chem. Chem. Phys. 8 (2006) 3083.